

Order-Disorder Transition in a Block Copolyurethane

Anthony J. Ryan*

Manchester Materials Science Centre, UMIST, Grosvenor Street, Manchester M1 7HS, U.K.

Christopher W. Macosko

Chemical Engineering and Materials Science, University of Minnesota,
421 Washington Avenue SE, Minneapolis, Minnesota 55455

Wim Bras

SERC, Daresbury Laboratory, Warrington WA4 4AD, U.K.

Received December 17, 1991; Revised Manuscript Received July 22, 1992

ABSTRACT: The temperature dependence of the thermal, rheological, and morphological properties of a block copolyurethane has been studied. The material investigated comprised hard segments formed from diphenylmethane diisocyanate (MDI) and 1,4-butanediol and soft segments based on a poly(oxyethylene-block-oxypropylene) diol of molecular weight 2300. Crystallinity of the hard segment was eliminated by using a 50:50 w:w mixture of 4,4'- and 2,4'-MDI. DSC data showed the existence of a microphase-separated structure in the copolymer which exhibited two glass transitions. Material quenched from above a third weak transition was homogeneous and showed only one intermediate glass transition. Dynamic mechanical analysis confirmed the glass transition behavior and showed a drop in modulus at elevated temperatures which was ascribed to the order-disorder transition of the microphase-separated block copolymer. The intensity-scattering vector data obtained in real-time small-angle X-ray scattering experiments showed a strong Bragg reflection at low temperatures which disappeared at elevated temperatures. The loss of the scattering peak occurred in the same temperature interval as the thermal and dynamic mechanical transitions and was also ascribed to the order-disorder transition ($T \approx 150^\circ\text{C}$). Further X-ray studies showed the location of the transition to be sensitive to molecular weight as predicted by theory.

I. Introduction

The unique combination of physical properties available from segmented block copolymers is related to their (micro)phase-separated structure. Typically, such polymers are formed from 4,4'-diphenylmethane diisocyanate (MDI) reacting with butane-1,4-diol (BDO) and a polyether diol (normally of molar mass 2000-4000). Copolyurethane materials, most specifically the model system mentioned above,¹ have been the subject of many experimental studies aimed at elucidating the relationships between composition (hard segment content), chemical microstructure, morphology and its development, and material properties. The structure of conventional copolyurethanes covers three basic size scales. The smallest size scale is that of the chain-chain dimensions (periodic over nanometers) and is concerned primarily with the nature of the crystallinity of hard segment units. The next size scale of interest is that of the microphase structure which is commonly periodic over a range of tens of nanometers and is set by the lengths of the blocks. The largest structural feature of note is the spherulitic texture of the crystallizable material which is periodic over a size scale of microns. In this paper we concentrate on the intermediate structure, that is, the microphase-separated structure of a block copolymer, by studying copolyurethanes with a noncrystallizable hard segment.

Since Cooper and Tobolsky² first published their results on the microphase-separated structure of segmented copolyurethanes, the nature of the driving force for microphase separation has been questioned. It is well established that at elevated temperatures there is a transition from a material with a well-defined morphology to an amorphous melt.³ Rapid quenching of the amorphous melt to liquid-nitrogen temperatures freezes in the amorphous structure which has been shown by DSC to have a single T_g .⁴ Thermal studies of copolyurethane systems are complicated by two factors: first, one of the

blocks (the hard segment) is capable of crystallization and the morphology is very sensitive to thermal history; second, there is a most probable distribution in the hard-segment sequence length. This results in a broadening of the transitions,⁵ and fractionation by the hard-segment length⁶ can occur during crystallization.

Eisenbach and co-workers,^{7a} Qin and co-workers,^{7b} and Christenson and co-workers⁸ have followed the pioneering work of Harrell⁹ and synthesized model copolyurethanes with monodisperse hard segments. These materials still have crystallizable hard segments, and if they are taken above the temperature where the urethane bond rearranges, they revert to having a most probable distribution in the hard-segment sequence length.¹⁰ Thus it is not possible to readily study the order-disorder transition in monodisperse materials as they rearrange in the temperature interval of interest. The microphase separation transition occurs at $\approx 200^\circ\text{C}$ for a typical MDI/BDO copolyurethane,¹¹ whereas the urethane bonds are considered unstable above $\approx 170^\circ\text{C}$.¹⁰

A well-characterized series of copolyurethanes have been studied by Koberstein and co-workers.^{3,6,11,12} The materials are based on pure 4,4'-MDI, BDO, and a poly(oxyethylene)-tipped poly(oxypropylene) diol. The materials have been synthesized in bulk and then annealed above the hard-segment melting point to ensure a most probable distribution in both hard-segment sequence length and global molecular weight. Thermal properties of these materials (such as the hard-segment melting point) depend strongly on the processing temperature.¹¹ Simultaneous FTIR/DSC¹² and synchrotron SAXS/DSC^{3,6,11} experiments have been successful in elucidating the origins of the processing-temperature-dependent nature of copolyurethanes. In particular, real-time synchrotron SAXS and WAXD¹¹ measurements of the kinetics of microphase separation and crystallization showed that the competition

between these two processes determined the final morphology.

The thermodynamics of diblock copolymer systems have been recently reviewed by Bates and Fredrickson.¹³ Block copolymer thermodynamics are complex and beyond the scope of this paper; however, a few major features of the mean-field theory according to Leibler¹⁴ and its development into the fluctuation theory of Fredrickson and Helfand¹⁵ will be highlighted. Due to the competition between the enthalpy and entropy of (micro)mixing, like monomer units will begin to aggregate at some temperature to form equilibrium microstructures. The relevant parameters in the theories used to describe this transition are f , the copolymer composition, and the product χN , where χ is the Flory-Huggins interaction parameter and N is the degree of polymerization. The weak first-order phase transition is known as the order-disorder transition, ODT, or the microphase-separation transition, MST. The ordered, equilibrium, mesophase structures formed are predicted to be either a body-centered cubic array of spheres, hexagonal close-packed rods, or alternating lamella. These structures are composition dependent and have been observed experimentally for diblock and triblocks by a number of workers.¹⁶⁻¹⁹ Bates and co-workers^{13,20-26} have used rheological and neutron scattering techniques to study the ODT in specially-synthesized aliphatic diblock copolymers. The ODT was observed as a step function in the in-phase component of the shear modulus, but in accordance with theoretical predictions of Fredrickson and Helfand¹⁵ there are only subtle changes in scattering patterns associated with the ODT for unoriented materials. Hashimoto, on the other hand, has investigated styrene-isoprene diblocks,^{27,28} styrene-isoprene-styrene triblocks,²⁹ and blends of diblocks and polystyrene homopolymer.³⁰ Time-resolved SAXS was used to follow the structure in mixtures of block copolymer and solvent (a neutral solvent was added to depress the ODT). In contrast to the studies mentioned above, Hashimoto observed the ODT as a deviation from linearity in a $1/I(q^*)$ versus $1/T$ plot as predicted by the mean-field theory of Leibler,¹⁴ and the Bragg spacing in the disordered state was lower than that in the ordered state. The discrepancies in the results of Bates and Hashimoto need to be resolved. The coarse-graining involved in Leibler's mean-field theory has been removed by the more detailed fluctuation theory of Fredrickson and Helfand;¹⁵ however, the question of which theory to use for analysis of experimental results remains.

The microphase-separation transition for multiblock copolymers is considered in the general mean-field theory presented by Hadzioannou and Benoit.³¹ However, there are no predictions available for the kind of mesophase geometry expected, especially in the case of crystallizable segmented copolymers such as copolyurethanes. Morphologies similar to those found in diblock copolymers have been reported in several microscopy investigations of copolyurethanes.^{32,33} Generally, the polydispersity (in both block length and global molecular weight) of segmented block copolymers means that imperfect microstructures form and bulk materials which pass from the bulk homogeneous (disordered) state through the MST into the ordered state are not normally at equilibrium; therefore, annealing has been observed to refine morphology.³⁴

In the present work attempts are made to follow the procedure of Bates and co-workers²⁰⁻²⁶ in combining the experimental techniques of rheology and radiation scattering to a copolyurethane containing 50% by weight of

amorphous polyurethane segments and 50% by weight of amorphous polyether segments. The rheological technique involves the measurement of the dynamic shear modulus in an oscillating parallel-plate mode, and, whereas Bates^{22,23,25} uses small-angle neutron scattering, the synchrotron SAXS technique was used to investigate real-time structural evolution during the heating and cooling of copolyurethanes.

II. Experimental Section

Synthesis. Copolyurethanes containing 50% hard segments were formed from three components: (i) an MDI-based diisocyanate (a 50:50 mixture of 2,4'- and 4,4'-diphenylmethane diisocyanate with an equivalent weight of 125; Isocyanate XZ-95263 from Dow Chemical), (ii) a polyether diol soft-segment oligomer (a 25% poly(oxyethylene)-tipped poly(oxypropylene) diol with $M_n = 2306$; Thanol E2103 from Texaco Chemicals), and (iii) a butanediol chain extender (obtained from Aldrich). No catalyst was used. All materials were used as received.

A mini-RIM machine with lever arm control was used to mix the chemicals. The machine and its operation are described in detail elsewhere.³⁵ The volume ratio of the mini-RIM machine was calibrated using liquid petroleum and enabled functional group stoichiometry to be maintained at $1.00 \pm 0.5\%$. The mixhead was based on the design of Macosko and McIntyre,³⁶ and this type of mixhead allows reactant recycle prior to impingement mixing. The Thanol E2103 and BDO were weighed, blended, degassed (at a vacuum of ~ 3 mmHg for 18 h at 60°C), and loaded into one side of the RIM machine, and the isocyanate was loaded into the other side. The tanks were then blanketed with nitrogen and the materials heated up to $60 \pm 5^\circ\text{C}$. Polyol Reynolds numbers were ~ 800 to ensure good mixing; the isocyanate Reynolds numbers were an order of magnitude greater. From the mixhead the reactive mixture was injected into an insulated paper cup to complete reaction under pseudo-adiabatic conditions. Prior to characterization the polymers were compression-molded for 10 min at 200°C and 15 tons of pressure; the molded sheets were then cooled to room temperature over a period of 4 h under pressure. Reaction injection molding was chosen over other synthetic techniques for its convenience. RIM does not involve the use of solvents and provides accurate stoichiometry for a number of bulk polymerizations which are intrinsically fast, due to being adiabatic, and thus less prone to macrophase separation. Compression molding at 200°C ensures that the whole sample has the same thermal history.

Size-Exclusion Chromatography. Molecular weights and distributions were obtained by injecting a dilute tetrahydrofuran solution (0.1–0.2% of polymer) into a stream of tetrahydrofuran (0.5 cm³/min) at 30°C which passed through two 10- μm , mixed-bed, cross-linked polystyrene columns on a Waters Model 150-C ALC/GPC equipped with a refractive index detector. Molecular weights are based upon a polystyrene calibration. The compression-molded material had $M_w = 15\,000$ and $M_w/M_n = 1.47$. Material removed from a SAXS cell after heating up to 240°C and exposure to the beam for 2 h had $M_w = 13\,000$ and $M_w/M_n = 1.56$. This reduction in M_w is discussed later.

Differential Scanning Calorimetry. DSC (TA 3000, Mettler Inc.) was used for heat capacity measurements to examine the polyether glass transition temperatures, T_g^s , and the polyurethane glass transition temperature, T_g^H . The values of T_g reported are taken at the midpoint of the transition. Sample masses of 10–20 mg were used at a heating rate of $10^\circ\text{C min}^{-1}$. The purge gas was dry nitrogen.

Dynamic Mechanical Spectroscopy. DMA data were obtained in the torsion rectangular mode at 1 Hz (System IV, Rheometrics Inc.) on test bars ($30 \times 10 \times 3$ mm) cut from compression-molded sheets. Measurements were shown to be strain insensitive in the region used (1% strain) and were made in a nitrogen atmosphere at a heating rate of 2°C min^{-1} from -100 to $+120^\circ\text{C}$. High-temperature ($T > 140^\circ\text{C}$) measurements were made in the parallel-plate mode. The plate size was 25 mm with a 1.5-mm gap. Measurements were made at 1 Hz and 4% strain in a nitrogen atmosphere at a heating rate of 2°C min^{-1} from 140 to 200°C .

Synchrotron Small-Angle X-ray Scattering. SAXS measurements were made on Beamline 8.2 on the Synchrotron Radiation Source (SRS) at the SERC Daresbury Laboratory, Warrington, U.K. The white radiation from the bending magnet is monochromated by a cylindrically bent Ge(111) monochromator with an asymmetric cut of 10.5° and consequently a horizontal compression ratio of 13:1 for the incoming beam. The distance from the tangent point of the storage ring to the monochromator is 20.0 m. The horizontal acceptance of the monochromator is approximately 5 mrad. The alignment is such that 1.52 \AA radiation is selected. By varying the bending radius, the radiation can be focused in the horizontal plane in the range of 0.2–4.5 m behind the sample stage.

An uncoated, fused-quartz mirror receives the monochromated radiation under a glancing angle of about 4 mrad. The mirror, which is cylindrically bent and 0.7 m in length, effectively cuts off all of the higher harmonics transmitted by the monochromator and focuses the radiation in the vertical plane. The beamline is kept under high vacuum, and four sets of slits are used for beam size definition and reduction of parasitic scatter. A highly collimated beam is produced with a typical cross section of $0.3 \times 4 \text{ mm}^2$ in the focal plane. With the SRS operating at 2 GeV and 200 mA, a flux of 4×10^{10} photons s^{-1} is generated at the sample position.

A vacuum chamber is placed between the sample and detector in order to reduce air scattering and absorption. Both the exit window of the beamline and the entrance window of the vacuum chamber are made from 15 μm mica; the exit window of the vacuum chamber is made from 10 μm Kapton film. A beamstop is mounted just before the exit window to prevent the direct beam from hitting the detector.

The camera is equipped with a multiwire quadrant detector. The quadrant detector has an opening angle of 70° and an active length of 0.2 m. This detector measures intensity in the radial direction and is only suitable for isomorphous scatterers. It has an advantage over single-wire detectors in that the active area increases radially. The spatial resolution of the detector is 500 μm , and it can handle count rates up to $\sim 250\,000$ counts s^{-1} .

The copolyurethane specimens for SAXS were prepared by placing disks, $\approx 2 \text{ mm}$ thick and $\approx 8 \text{ mm}$ in diameter, cut from compression-molded sheets, in a cell comprising a 2 mm-thick brass spacer and 10 μm mica windows. Loaded cells were fitted with a J-type thermocouple and placed in a Linkam hot-stage mounted on the optical bench. The silver heating block of the hot-stage contains a $4 \times 1 \text{ mm}$ conical hole which allows the transmitted and scattered X-rays to pass through unhindered. A heating rate of $1.8^\circ\text{C min}^{-1}$ was used.

The scattering pattern from an oriented specimen of wet collagen (rat-tail tendon) was used to calibrate the sample-to-detector distance. Parallel-plate ionization detectors placed before and after the sample cell record the incident and transmitted intensities, thus enabling changes in the specimen attenuation factors (a function of transmission and thickness) to be monitored continuously. The experimental data were corrected for background scattering (subtraction of the scattering from the camera, hot stage, and an empty cell), sample thickness and transmission, and the positional alinearity of the detector.

III. Results and Discussion

Differential Scanning Calorimetry. Figure 1 presents the DSC results for the block copolyurethane. The upper DSC trace is that of the compression-molded material showing two major transitions, the soft-segment glass transition temperature, T_g^S , at -45°C and the hard-segment glass transition temperature, T_g^H , at 93°C . The value of T_g^S is approximately 20°C higher than the T_g observed for the pure soft-segment oligomer,³⁷ indicating that there is some mixing of hard segments in the soft-segment microphase, whereas T_g^H is in good agreement with the T_g of 99°C observed for a pure hard segment formed in solution.³⁸ A third, less intense, endothermic transition is observed at $\approx 145^\circ\text{C}$, and this is labeled as "ODT?". The sample was shown to be completely amorphous by wide-angle diffraction experiments, and so

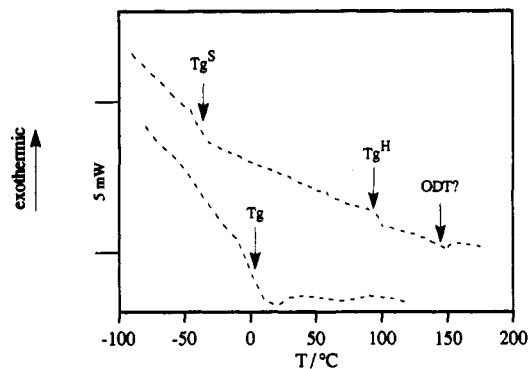


Figure 1. DSC curves for a compression-molded copolyurethane containing 50% amorphous hard segments. Upper curve, compression-molded material. Lower curve, the same material quenched from 170°C .

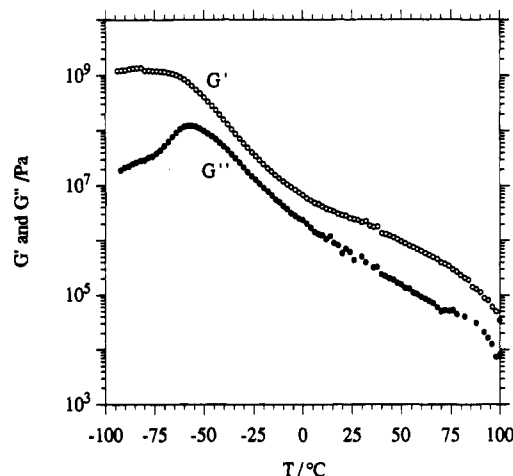


Figure 2. Torsional storage modulus, G' , and loss modulus, G'' , data in the temperature interval -100 to $+100^\circ\text{C}$ for a compression-molded copolyurethane containing 50% amorphous hard segments.

this weak feature is not associated with crystalline melting of the hard segment. The endothermic nature of the transition indicates that it is a mixing event and not the exothermic breakdown of hydrogen-bonded urethane hard segments^{6,7} previously associated with the order-disorder transition. Furthermore, FT-IR of similar polyurethanes⁸ show no hydrogen-bonded carbonyl absorbances above 120°C .

After heating to 200°C , the DSC pan was removed from the measuring head, rapidly quenched into liquid nitrogen, and then replaced in the measuring head at $\approx 100^\circ\text{C}$. The lower DSC trace is that of the quenched material, and, in contrast to the compression-molded material, it has only one thermal transition, located at $T_g = 5^\circ\text{C}$ in Figure 1. This transition is ascribed to the T_g of the homogeneous block copolymer and is in good agreement with the value of 8°C predicted by the Fox equation:

$$1/T_g = w^S/T_g^S + w^H/T_g^H$$

where w^S and w^H are the weight fractions and T_g^S and T_g^H are the glass transitions of the pure soft and hard segments, respectively.

Dynamic Mechanical Spectroscopy. The low-frequency (1 Hz), low-temperature, shear modulus data are presented in Figure 2. The polyether glass transition, T_g^S , is observed as a peak in G'' at $\approx -60^\circ\text{C}$. The transition extends over a temperature interval (-60 to -20°C) where the storage modulus decreases by 2 orders of magnitude. Between 0 and 80°C there is a rubbery plateau in the shear modulus, and at temperatures approaching 100°C

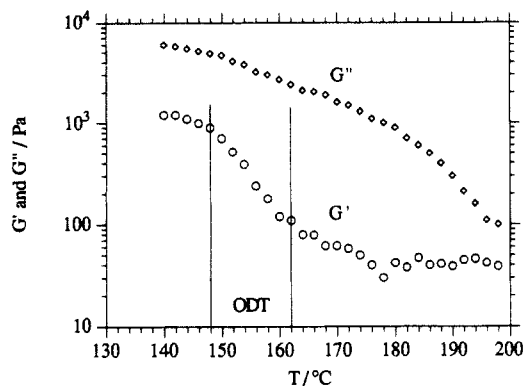


Figure 3. Parallel-plate storage modulus, G' , and loss modulus, G'' , data in the temperature interval 140–200 °C for a compression-molded copolyurethane containing 50% amorphous hard segments.

the copolyurethane enters another transition, which as indicated by DSC is ascribed to T_g^H , where the sample became too soft to measure G' and G'' in torsion.

The low-frequency (1 Hz), high-temperature, shear modulus data are presented in Figure 3, where there is a continuous drop of 1 order of magnitude in the observed value of G' over the temperature interval 148–163 °C. The corresponding change in G'' over this temperature interval is not as great in magnitude, and this is in good agreement with the observations of Bates and co-workers on diblock copolymers.²⁶ Monodisperse block copolymers have been shown to have an ODT which is characterized by a discontinuous drop in the low-frequency, dynamic elastic shear modulus, G' , consistent with the first-order nature of this transition.^{21,23,24} Conversely, bimodal mixtures of block copolymers have a broad transition in G' , and this has been rationalized by Bates and co-workers²⁷ in the context of classic, two-component, liquid–solid, phase behavior. Such an analogy would not be entirely appropriate here where there are comparatively broad distributions of global molecular weight and hard-segment sequence length. However, the physical picture of a large region of complete liquid-state and solid-state miscibility of the block copolymer chains with a broad distribution of lengths, with a biphasic region bounded by liquidus and solidus lines, is very useful. Within the biphasic region an ordered phase, rich in high molar mass (high hard-segment sequence length) material, will exist in equilibrium with a disordered phase rich in low molar mass (low hard-segment sequence length) material. Increasing or decreasing the temperature produces a continuous shift in the volume fractions of the solid and liquid phases and a consequent continuous shift in G' . Segregation of polydisperse block copolymers into ordered and disordered phases according to chain length was invoked by Koberstein^{6,11,12} to explain FTIR, DSC, and SAXS data in the initial work on the dynamics of copolyurethane morphology in the 1980s.

Synchrotron Small-Angle X-ray Scattering. Time-resolved SAXS data were collected during heating and cooling experiments. Figure 4 is a three-dimensional plot of intensity, $I(q, T)$, versus scattering vector, q , versus temperature, T , in the temperature interval 70–190 °C for the compression-molded copolyurethane. Qualitatively the low-temperature diffraction patterns are typical of a microphase-separated block copolymer with a maximum in I at a scattering vector $q_{\max} \approx 0.04 \text{ \AA}^{-1}$. The magnitude of $I(q_{\max})$ increases with increasing T , most noticeably in the temperature interval 100–130 °C. Between 140 and 150 °C there is a distinct change in the scattering

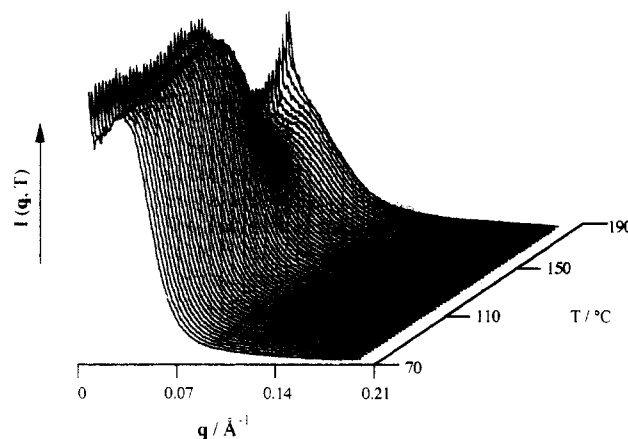


Figure 4. Three-dimensional plot of intensity, $I(q, T)$, versus scattering vector, q , $0 < q < 0.21 \text{ \AA}^{-1}$, versus temperature, T , in the temperature interval 70–190 °C for the higher molecular weight compression-molded copolyurethane containing 50% amorphous hard segments.

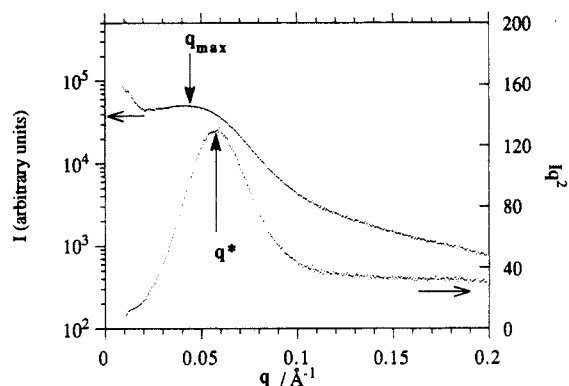


Figure 5. Relative intensity, $I(q)$, and Lorentz-corrected relative intensity, $I(q)q^2$, versus scattering vector, q , showing the position of q_{\max} and q^* for the higher molecular weight compression-molded copolyurethane at 70 °C.

patterns: the peak in $I(q)$ disappears and is replaced by a shoulder on a decaying $I(q)$ curve. At the highest temperatures used the shoulder becomes a less dominant feature and the scattering at very low angle increases, most likely due to bubble formation. Some small voids could be observed in materials cooled down and removed from the cell.

The initial form of the data is as a plot of intensity (I) versus scattering vector (q); although there is a peak in the intensity curve, the lamella nature of the copolyurethane's morphology means that the Lorentz correction³⁹ (q^2) must be applied to the intensity before spatial information is extracted in the form of a one-dimensional spacing. The peak in the Lorentz-corrected scattering curve (q^*) may be analyzed according to Bragg's law ($1 - d = 2\pi/q^*$) to derive the $1 - d$ spacing. This is illustrated in Figure 5, a plot of $I(q)$ and $I(q)q^2$ versus q at 70 °C. The peak value from $I(q)$ versus q overestimates³⁹ the d spacing at $\approx 150 \text{ \AA}$, whereas the peak value from $I(q)q^2$ versus q gives a $1 - d$ spacing of $\approx 110 \text{ \AA}$. The high quality of the experimental data is apparent from the low variance at high values of q ; this is due to the greater active area of the quadrant detector when compared with a linear detector.

The invariant (Q) is a linear function of the square of the electron density difference ($\langle \eta^2 \rangle$) between the soft

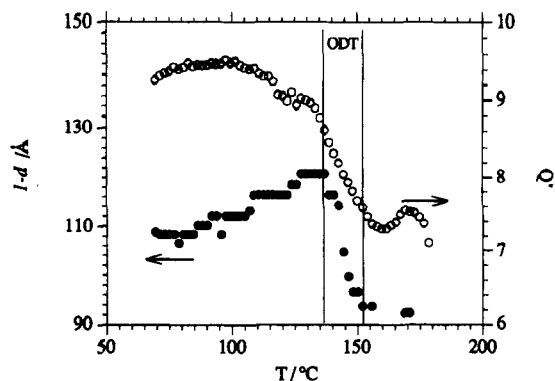


Figure 6. Relative invariant and $1-d$ spacing versus temperature for the higher molecular weight compression-molded copolyurethane containing 50% amorphous hard segments.

segment (polyether) and hard segment (polyurethane) rich phases and is obtained from the integral

$$\langle \eta^2 \rangle = \frac{Q}{2\pi i_e} = \frac{1}{2\pi i_e} \int_0^\infty I(q) q^2 dq$$

where i_e is the Thompson scattering factor. The quantity Q is known as the invariant being independent of the size or shape of the structural heterogeneities. The absolute value of the invariant requires absolute intensity measurements, thermal background subtraction, and extrapolation to $q = 0$ and ∞ and is computationally difficult to achieve. The major contribution to the experimental invariant can be used to characterize structure development, as well as the degree of microphase separation, and is readily assessed by Simpson's rule integration of the $I(q) q^2$ versus q curve between experimental limits.^{3,11} A relative invariant, Q' , has been calculated by summation of the area under the $I(q) q^2$ versus q curve between the first reliable data point, $q = 0.01 \text{ \AA}^{-1}$, and the region in which $I(q) q^2$ becomes constant, that is, at $q = 0.18 \text{ \AA}^{-1}$. Due to the relative nature of the intensity measurement, the value of Q' is also only relative with arbitrary units.

Figure 6 is a plot of $1-d$ and Q' versus T for the compression-molded material, and there are three distinct regions to the curves. $1-d$ increases linearly with T , and the magnitude of Q' shows a broad maximum in the temperature interval 70–135 °C. Between ~135 and 155 °C there is a linear reduction in both $1-d$ and Q' , whereas above 160 °C $1-d$ is constant at ~90 Å and Q' oscillates between 7.1 and 7.5. The behavior of the $1-d$ spacing of the copolyurethane studied here differs greatly from that of previous studies on copolyurethanes with semicrystalline hard segments where the onset of hard-segment melting is associated with an increase in $1-d$ as individual lamella melt and immediately mix.¹¹ The linear increase of $1-d$ with T , at $T \leq 130$ °C, allows calculation of a coefficient of thermal expansion. The value obtained by fitting a straight line through a $\partial(1-d)/(1-d)$ versus T curve is $\approx 6.9 \times 10^{-4} \text{ K}^{-1}$. This value is consistent with the coefficient of thermal expansion of $6.0 \times 10^{-4} \text{ K}^{-1}$ given by van Krevelen⁴⁰ for poly(oxypropylene) and that of $6.5 \times 10^{-4} \text{ K}^{-1}$ calculated, using van Krevelen's method,⁴⁰ for the hard segment. The broad maximum observed in Q' is a product of the increase in $1-d$ and $I(q^*)$. The sharp fall in Q' and $1-d$ is associated with the qualitative change in the scattering patterns from those with a peak in $I(q)$ to those with a shoulder in $I(q)$. This region has been labeled as ODT in Figure 6 and covers the temperature interval 135–155 °C. It is conceivable that the shoulder, observed above 150 °C in the scattering patterns of Figure 4, is due to correlation hole scattering as discussed by de Gennes.⁴¹

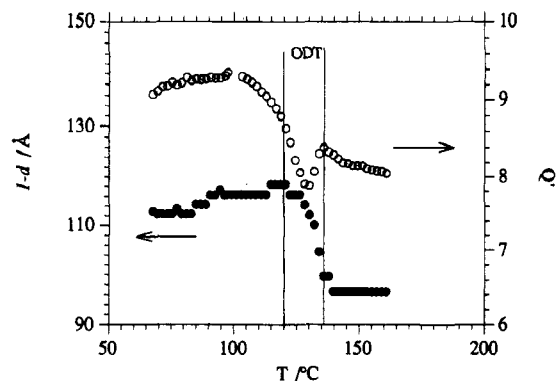


Figure 7. Relative invariant and $1-d$ spacing versus temperature for the lower molecular weight copolyurethane containing 50% amorphous hard segments.

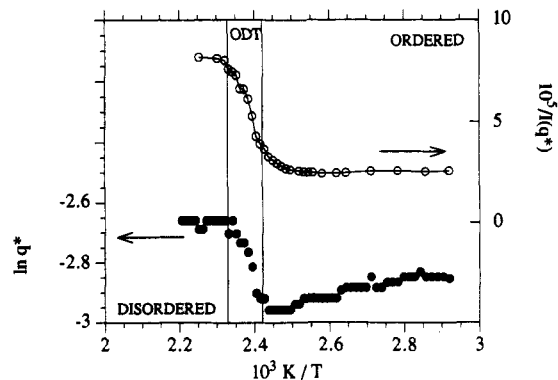


Figure 8. Leibler¹⁴ plot of the reciprocal of the peak scattered intensity, $1/I(q^*)$, and the logarithm of the peak scattering wave vector, $\ln(q^*)$, versus reciprocal temperature, T , for the higher molecular weight compression-molded copolyurethane containing 50% amorphous hard segments.

Figure 7 is a plot of $1-d$ and Q' versus T for the lower molecular weight copolyurethane that had been in the beam for 2 h and run up to 240 °C. The extreme conditions to which the material had been exposed caused the degradation in molecular weight; considering the high radiation doses and temperatures involved, the reduction in molecular weight is small but significant. The overall behavior is qualitatively similar to that of the compression-molded material. The sharp fall in Q' and $1-d$ is associated with the qualitative change in the scattering patterns from those with a peak in $I(q)$ to those with a shoulder in $I(q)$. This region has been labeled as ODT in Figure 7 and covers the temperature interval 122–135 °C. The molecular weight dependence of the ODT, observed experimentally in the present study, is one of the key features of the theories of Leibler,¹⁴ Benoit and Hadzioannou,³¹ Fredrickson and Helfand,¹⁵ Fredrickson and Milner,⁴² and most recently Fredrickson, Milner, and Leibler.⁴⁵

In order to compare our experimental results with the mean-field and fluctuation theories of block copolymer thermodynamics, $\ln(q^*)$ and $1/I(q^*)$ are plotted against $1/T$ (Figure 8), in the manner suggested by Leibler¹⁴ and Bates and Fredrickson.¹³ In common with the recent work of Hashimoto,^{27,30} but in contrast to the recent data on diblock copolymers published by Bates,^{23,24,25} $\ln(q^*)$ exhibits a strong feature at the ODT. The linear decrease in $\ln(q^*)$ with T has been analyzed above and corresponds to thermal expansion of the lamellar morphology. Interestingly, a theory of the thermodynamics of random copolymer melts has been recently published⁴² with the result that "the mesophase structure gets coarser as the temperature is raised"; this would correspond with an increase in the $1-d$ spacing (or a decrease in $\ln(q^*)$) for our random multiblock system. Thus the experimental

observations of an increase in the $1 - d$ spacing could be explained by either the coefficient of thermal expansion or the mesophase coarsening predicted by theory^{42,45} (however, the coincidence of the change in $1 - d$ and the expansion coefficients favors the former). The large step change in $\ln(q^*)$ is associated with the ODT and shows a contraction of the observed interdomain spacing which could be due to the chains adopting near-Gaussian conformations above the ODT as opposed to the stretched conformations which would have been present before the ODT. Cooper and co-workers⁴³ have observed, by SANS, that the radius of gyration, R_g , of the labeled soft-segment block of a copolyurethane is reduced on passing through the MST, and the transition from Gaussian to stretched coil conformations has recently been discussed for model diblocks.²⁵ The reciprocal peak intensity varies nonlinearly with inverse temperature and has a sigmoidal shape which is at variance with the theories of the ODT for monodisperse diblock copolymers. The ODT is marked on the curve as the temperature interval covering the large step change in $\ln(q^*)$ and encompasses the majority of the change in $1/I(q^*)$.

One important question raised about segmented block copolyurethanes is whether or not they can really be said to possess an ordered phase, that is, a phase with long-range order. Extensive review of the literature on SAXS of polyurethane has not produced any reference giving a scattering pattern which shows higher order reflections from the main peak.^{3,6-8,11,12,32,33,43,44} If copolyurethanes really possessed a long-range ordered phase with sharp phase boundaries, similar to that observed in model styrene–diene diblocks, at least one of the systems with a lamellar morphology should have been asymmetric enough that the second-order peak would not cancel out. Even the materials with nominally rodlike (hexagonal) or spherical morphologies fail to give higher orders.^{32,33} A SAXS pattern taken from Kraton TR1107 styrene–butadiene–styrene triblock, using the same camera as that for the copolyurethanes discussed here, gave a readily observable fifth-order reflection. In addition, SAXS patterns taken from SIS diblocks using a Kratky camera²⁷ show many higher order reflections. Thus the nature of microphase-separated copolyurethanes is that of a material with spatial correlations over the size scale determined by the principle Bragg peak but which possesses no long-range order, giving rise to coherence and higher order reflections. TEM micrographs of polyurethane show the short-range order of plates, rods, and spheres,^{32,33} but with the exception of one HVEM micrograph,³⁴ materials with a regular structure over more than five morphological repeats are not observed. It has been pointed out (by a reviewer) that the diffuse phase boundaries will also smear out higher order reflections from a structure with long-range order, and this could be the case here. Recent theoretical work,^{42,45} however, predicts that “microphases in random copolymer melts will typically lack long-range order and that the microphase period should exhibit extreme temperature sensitivity near the ODT”.

Thus the existence of the ODT is beyond doubt, but an unambiguous statement on the existence of a long-range ordered phase in multiblock copolyurethanes is difficult to make. The reasons why “crystallographic” (long-range) order is not observed in these copolymers are due to the need for a multiblock chain to take part in a large number of domains, and the formation of long-range order would require an enormous cooperativity which is most likely precluded by entropic considerations.^{13,45}

IV. Summary and Conclusions

Three independent experimental techniques have been used to investigate the high-temperature transition behavior of a copolyurethane containing 50% by weight of amorphous polyurethane segments and 50% by weight of amorphous polyether segments. The DSC data show the material to have a well-segregated microstructure, with glass transition temperatures corresponding to the two segments and a low-magnitude thermal transition at $\sim 150^\circ\text{C}$ which could be attributed to the ODT. Material quenched from above the ODT has only one intermediate glass transition temperature. Rheological experiments show a continuous drop of an order of magnitude in the observed value of G' over the temperature interval $148\text{--}163^\circ\text{C}$. The sharp fall in Q' and $1 - d$ in the temperature interval $140\text{--}160^\circ\text{C}$ is associated with the qualitative change in the scattering patterns from those with a peak in $I(q)$ to those with a shoulder in $I(q)$. The extreme temperature sensitivity of the $1 - d$ spacing close to the ODT is predicted by theory.⁴⁵ The shoulder in the scattering pattern observed above 150°C could be due to correlation hole scattering. A material of lower molecular weight has also been investigated by SAXS; its behavior is qualitatively similar to that described above with an ODT that is approximately 20°C lower than that of the compression-molded material.

Generally a broad transition is observed, the physical picture close to the ODT being one of complete liquid-state and solid-state miscibility of the block copolymer chains with a broad distribution of lengths, with a biphasic region bounded by liquidus and solidus lines. Within the biphasic region a high molar mass rich ordered phase will exist in equilibrium with a low molar mass rich disordered phase. Increasing or decreasing the temperature produces a continuous shift in the volume fractions of the solid (ordered) and liquid (disordered) phases and a consequent continuous shift in G' and the SAXS patterns. Segregation of polydisperse block copolymers into ordered and disordered phases according to chain length has been invoked previously by Koberstein and co-workers¹³ to explain FTIR, DSC, and SAXS data for copolyurethanes and, more recently, by Bates and co-workers²⁶ to account for the rheological behavior of mixtures of diblock copolymers. Their interpretation of the behavior of block copolymer mixtures is supported by our experimental data. Finally the behavior of the $1 - d$ spacing (q^*) close to the ODT, observed in our scattering studies of these random multiblock copolymer melts, follows closely that predicted in a recent theoretical development by Fredrickson, Milner, and Leibler.⁴⁵

Acknowledgment. Todd Bergstrom performed the DMS spectroscopy and was financially supported by the NSF. SERC provided the synchrotron SAXS beam-time and financial support for the SAXS experiments. A.J.R. was supported by a NATO Fellowship for part of this work. Frank Bates, Mike Elwell, Jeff Koberstein, John Stanford, and Wayne Willkomm critically discussed the results and the manuscript. Glenn Fredrickson kindly provided a copy of ref 45 prior to its publication. We are grateful for the constructive criticism of the anonymous reviewers.

References and Notes

- 1) Macosko, C. W. *RIM Fundamentals*; Oxford University Press: New York, 1989.
- 2) Cooper, S. L.; Tobolsky, A. V. *J. Appl. Polym. Sci.* **1966**, *10*, 1837.

- (3) Koberstein, J. T.; Russell, T. P. *Macromolecules* **1986**, *19*, 714.
- (4) Camberlin, Y.; Pascault, J. P. *J. Polym. Sci., Polym. Chem. Ed.* **1983**, *27*, 415.
- (5) Eisenbach, C. D.; Baumgartner, M.; Günter, C. *Polym. Prepr. (Am. Chem. Soc., Div. Polym. Chem.)* **1985**, *26* (2), 7.
- (6) Leung, L. M.; Koberstein, J. T. *J. Polym. Sci., Polym. Phys. Ed.* **1985**, *23*, 1883.
- (7) (a) Eisenbach, C. D.; Baumgartner, M.; Günter, C. *Advances in Elastomers and Rubber Elasticity*; Lal, J., Mark, J. E., Eds.; Plenum Publishing Corp.: New York, 1987; p 51. (b) Qin, Z. Y.; Macosko, C. W.; Wellinghof, S. T. *Macromolecules* **1985**, *18*, 553.
- (8) (a) Christenson, C. P.; Harthcock, M. A.; Meadows, M. D.; Spell, H. L.; Howard, W. L.; Creswick, M. W.; Guerra, R. E.; Turner, R. B. *J. Polym. Sci., Polym. Phys. Ed.* **1986**, *24*, 1401. (b) Lee, H. S.; Wang, Y. K.; Hsu, S. L. *Macromolecules* **1987**, *20*, 2089.
- (9) Harrell, L. L. *Macromolecules* **1969**, *2*, 607.
- (10) Yang, W. P.; Macosko, C. W.; Wellinghof, S. T. *Polymer* **1986**, *27*, 1325.
- (11) Galambos, A. F.; Russell, T. P.; Koberstein, J. T. *Proceedings of the 18th NATAS Conference*, San Diego, CA, Sept 24-27, 1989; Paper 35.
- (12) Leung, L. M.; Koberstein, J. T. *Macromolecules* **1986**, *19*, 706.
- (13) Bates, F. S.; Fredrickson, G. H. *Annu. Rev. Phys. Chem.* **1990**, *41*, 525.
- (14) Leibler, L. *Macromolecules* **1980**, *13*, 1602.
- (15) Fredrickson, G. H.; Helfand, E. *J. Chem. Phys.* **1987**, *87*, 697.
- (16) Hadziioannou, G.; Skoulios, A. *Macromolecules* **1982**, *15*, 271.
- (17) Price, C.; Lally, T. P.; Watson, A. G.; Woods, D.; Chow, M. T. *Br. Polym. J.* **1972**, *4*, 413.
- (18) Hashimoto, T.; Nagatoshi, K.; Todo, A.; Hasegawa, H.; Kawia, H. *Macromolecules* **1974**, *7*, 364.
- (19) Alward, D. B.; Kinning, D. J.; Thomas, E. L.; Fetters, L. J. *Macromolecules* **1986**, *19*, 215.
- (20) Bates, F. S.; Bair, H. E.; Hartney, M. A. *Macromolecules* **1984**, *17*, 1987.
- (21) Bates, F. S. *Macromolecules* **1984**, *17*, 2607.
- (22) Bates, F. S.; Hartney, M. A. *Macromolecules* **1985**, *18*, 2478.
- (23) Bates, F. S.; Rosedale, J. H.; Fredrickson, G. H. *J. Chem. Phys.* **1990**, *92*, 6255.
- (24) Rosedale, J. H.; Bates, F. S. *Macromolecules* **1990**, *23*, 2329.
- (25) Almdal, K.; Rosedale, J. H.; Bates, F. H.; Wignall, G. D.; Fredrickson, G. H. *Phys. Rev. Lett.* **1990**, *65*, 1112.
- (26) Almdal, K.; Rosedale, J. H.; Bates, F. S. *Macromolecules* **1990**, *23*, 4336.
- (27) Hashimoto, T. In *Physical Optics of Dynamic Phenomena and Processes in Macromolecular Systems*; Sedlacek, B., Ed.; Walter de Gruyter & Co.: Berlin, Germany, 1985; p 233.
- (28) Hashimoto, T.; Suehiro, S.; Shibayama, M.; Saijo, K.; Kawai, H. *Polym. J.* **1980**, *13*, 501.
- (29) Fujimura, M.; Hashimoto, H.; Kurahashi, K.; Hashimoto, T.; Kawai, H. *Macromolecules* **1981**, *14*, 1196.
- (30) Tanaka, H.; Hashimoto, T. *Macromolecules* **1991**, *24*, 5713.
- (31) Benoit, H.; Hadziioannou, G. *Macromolecules* **1988**, *21*, 1449.
- (32) Chen-Tsai, C. H. Y.; Thomas, E. L.; MacKnight, W. J.; Schneider, N. S. *Polymer* **1986**, *27*, 659.
- (33) Li, C.; Goodman, S. L.; Albrecht, R. M.; Cooper, S. L. *Macromolecules* **1988**, *21*, 2367.
- (34) Goodman, S. L.; Li, C.; Cooper, S. L.; Albrecht, R. M. *Proceedings of the 46th Annual Meeting of the Electron Microscopy Society of America*; San Francisco Press Inc.: San Francisco, CA, 1988; pp 936-7.
- (35) Mikkelsen, K.; Macosko, C. W. *J. Cell Plast.* **1989**, *21*, 29.
- (36) Macosko, C. W.; McIntyre, D. B. U.S. Patent 4,473,531, 1984.
- (37) Camargo, R. E.; Macosko, C. W.; Tirrell, M.; Wellinghof, S. T. *Polymer* **1985**, *26*, 1145.
- (38) Stamboulis, A. M.Sc. Dissertation, Victoria University of Manchester, 1991.
- (39) Cullity, D. B. *Elements of X-ray Diffraction*, 2nd ed.; Addison-Wesley: Reading, MA, 1978; pp 127-131.
- (40) van Krevelen, D. W. *Properties of Polymers: Correlations with Chemical Structure*, 3rd ed.; Elsevier: Amsterdam, The Netherlands, 1991.
- (41) de Gennes, P.-G. *J. Phys. (Paris)* **1975**, *31*, 235. de Gennes, P.-G. *Scaling Concepts in Polymer Physics*; Cornell University Press: Ithaca, NY, 1979.
- (42) Fredrickson, G. H.; Milner, S. T. *Phys. Rev. Lett.* **1991**, *67*, 835.
- (43) Miller, J. A.; Cooper, S. L.; Han, C. C.; Pruckmeyer, G. *Macromolecules* **1984**, *17*, 1063. Miller, J. A.; Pruckmeyer, G.; Epperson, J. E.; Cooper, S. L. *Polymer* **1985**, *26*, 1917.
- (44) Wilkes, G. L.; Tayagi, D. *Polym. Eng. Sci.* **1986**, *26*, 1371.
- (45) Fredrickson, G. H.; Milner, S. T.; Leibler, L., submitted to *Macromolecules*.